High peak-power mid-infrared $ZnGeP_2$ optical parametric oscillator pumped by a Tm:fiber master oscillator power amplifier system

Martin Gebhardt,[1,2,*] Christian Gaida,[1,2] Pankaj Kadwani,[1,3] Alex Sincore,[1] Nils Gehlich,[1,4] Cheonha Jeon,[1] Lawrence Shah,[1] and Martin Richardson[1]

[1]Townes Laser Institute, CREOL, University of Central Florida, 4000 Central Florida Blvd., Orlando, Florida 32816, USA

[2]Friedrich-Schiller University Jena, Max-Wien-Platz 1, D-07743 Jena, Germany

[3]Currently with IPG Photonics Corporation, Oxford, Massachusetts 01540, USA

[4]Fraunhofer Institute for Laser Technology, Aachen, Germany

*Corresponding author: martin.gebhardt@uni-jena.de

Received November 21, 2013; revised January 14, 2014; accepted January 20, 2014; posted January 24, 2014 (Doc. ID 201469); published February 21, 2014

We report on the utilization of a novel Tm:fiber laser source for mid-IR $ZnGeP_2$ (ZGP) optical parametric oscillator (OPO) pumping. The pump laser is built in a master oscillator power-amplifier configuration delivering up to 3.36 W of polarized, diffraction limited output power with 7 ns pulse duration and 4 kHz repetition rate. This corresponds to a peak power of ~121 kW and a pulse energy of ~0.84 mJ. With this source, we generated 27.9 kW of total mid-IR peak power in a doubly resonant oscillator (DRO) configuration. This is, to the best of our knowledge, the highest ever demonstrated mid-IR peak power from a directly Tm:fiber laser pumped ZGP OPO. Moreover, a DRO output with about 284 μJ of total mid-IR pulse energy was demonstrated using 100 ns pump pulses. The wavelength tuning of the idler was extended to 6 μm with lower output power in another OPO experiment.

OCIS codes: (060.5295) Photonic crystal fibers; (190.4970) Parametric oscillators and amplifiers.
http://dx.doi.org/10.1364/OL.39.001212

The mid-IR wavelength range is of high interest for a wide range of applications due to the numerous vibrational molecular transitions in the 3–10 μm regime. Moreover, this spectral region contains several low-loss propagation windows enabling long-range "eye safe" remote sensing applications. Similarly, unique materials processing applications are possible by taking advantage of mid-IR absorption resonances [1]. The goal of this work is to develop a relatively straightforward and robust system providing broad wavelength tunability in the mid-IR with high peak power/high energy in order to conduct materials ablation experiments both "on" and "off" resonance.

Due to the lack of energetic pulsed laser sources directly operating in the mid-IR, nonlinear frequency conversion is a widely used method to generate radiation in this regime. In particular, $ZnGeP_2$ (ZGP) is an attractive nonlinear material for multi-watt mid-IR optical parametric oscillator (OPO) due to its high nonlinearity (75 pm/V) and high damage threshold (~1–2 J/cm^2) [2] as well as good optical, thermal and mechanical properties. Although ZGP has a low absorption coefficient ranging from 2 to 8 μm, there is strong absorption for wavelengths shorter than 1.95 μm [2], making direct pumping by Nd or Yb laser systems impossible.

Early ZGP OPO systems have been pumped using a range of sources including cryogenically cooled diode-pumped Ho-based solid-state lasers [3], flash-lamp pumped Er-based solid-state lasers [4], and the output of another OPO [5]. More recently, room temperature Ho:YAG [6] and Ho:YLF [7] solid-state lasers pumped by Tm:fiber lasers have become the standard. A more elegant way is to directly pump the ZGP OPO with a Tm:fiber laser. This approach has been successfully demonstrated reaching more than 2–3 W of mid-IR output power [8,9]. Such a Tm:fiber pump laser must provide high peak power with near diffraction-limited beam quality, narrow spectral linewidth, and a high polarization extinction ratio to drive the nonlinear conversion efficiently. These requirements can be fulfilled by Tm:fiber laser systems that have been developed in the last years.

However, pulsed fiber lasers are limited by nonlinearities associated with the tight confinement and the long interaction length inherent in the fiber geometry. As with Yb:fiber lasers, the development of photonic crystal fibers (PCF), offering signal mode field areas beyond 1000 μm^2 doped with Tm^{3+} ions, has enabled high-energy Tm:fiber lasers with nearly perfect beam quality and linearly polarized output [10]. In pulsed operation our group has demonstrated excellent Q-switched laser performance [11]. Due to this development it is now possible to extract higher peak powers from the fibers and thus, exceed the output peak powers demonstrated in previous works that use Tm:fiber lasers as a pumping source for a ZGP OPO.

Here we utilize a master oscillator power amplifier (MOPA) system consisting of a Tm:fiber Q-switched oscillator followed by two amplifier stages based on flexible Tm:PCFs. The PCFs (fabricated by NKT Photonics A/S) are the same as used in [10,11]. As illustrated in Fig. 1, the oscillator is based on a ~4 m long Tm doped polarization maintaining single-mode step index fiber with 10/130 μm core/cladding diameters (Nufern Inc.). A 35 W, 793 nm diode laser (DILAS Diode Laser Inc.) pumps the oscillator which is Q-switched by an acousto-optic modulator, (NEOS Technologies). The pump diode is spliced to the active fiber using a $(2+1):1$ fiber combiner (ITF Labs, 3S Photonics S.A.S.). The Q-switch portion of the cavity consisted of free-space optics including a half-wave plate and polarizing beam splitter (PBS) for polarization control and a

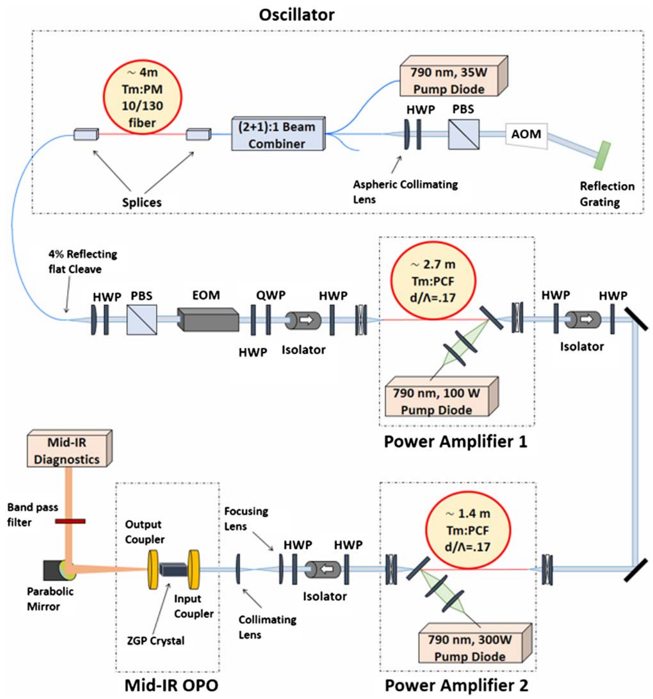

Fig. 1. System schematic shows the pump laser, consisting of a Q-switched oscillator and two power amplifiers; the optical isolator, half-wave plate (HWP), and telescope to pump the OPO; the linear OPO cavity; and mid-IR diagnostics.

600 l/mm gold-coated reflection grating for wavelength control. The oscillator generates ~100 ns pulses with ~25 μJ pulse energy at 20 kHz repetition rate. The 10 dB spectral linewidth is less than 1 nm, centered at ~1980 nm.

An electro-optic modulator (FastPulse Technologies) is used to reduce the pulse repetition rate to 1–20 kHz and slice out a portion of the 100 ns pulses, as short as 6.5 ns, for subsequent amplification. A repetition rate of 4 kHz was chosen based on the ~500 μs fluorescence lifetime of the upper laser level ($^3F_4$) in Tm doped silica fibers [12] in order to achieve high peak powers and pulse energies with low amplified spontaneous emission (ASE) content. An optical isolator is used to prevent feedback to the oscillator. Both amplifiers consist of flexible Tm:PCF sections of different length. The first amplifier fiber is ~2.7 m long and free-space pumped in a counter-propagating geometry with a 100 W, 793 nm diode laser (DILAS Diode Laser Inc.). The output of the first amplifier passes through a free-space optical isolator and is coupled into the second amplifier consisting of a ~1.4 m length of fiber pumped by a 300 W, 793 nm diode laser (LIMO Lissotschenko Mikrooptik GmbH) in a similar free-space, counter-propagation geometry as the first amplifier. The final output is collimated and passes through another optical isolator to pump the OPO.

The pulses are amplified to ~280 μJ pulse energy at ~7 ns pulse duration in the first PCF amplifier. After the final isolator the maximum usable, polarized power output is 3.36 W. This corresponds to ~0.84 mJ pulse energy at ~7 ns pulse duration or ~121 kW peak power. The output power of the final amplifier stage shows no roll off (Fig. 2). The maximum diode pump power for the second amplifier was limited to 45 W by melting

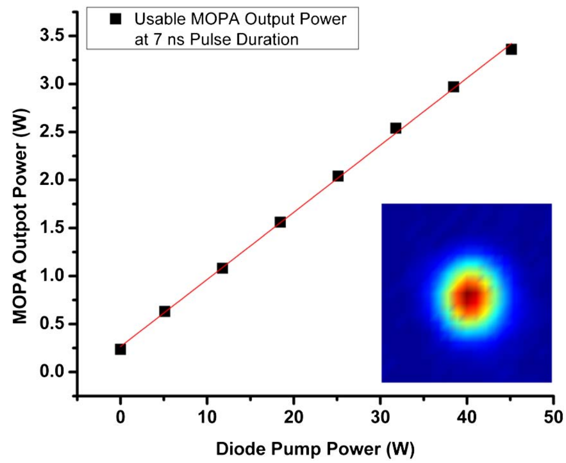

Fig. 2. Average output power from the final amplifier relative to diode pump power corresponds to a slope efficiency of 7%. Inset: far-field beam profile at highest output power.

of the PCF polymer coating due to the heat induced by the strong thermal load at the pump/output end of the fiber. The fiber was air-cooled and its pump end was mounted on a water-cooled aluminum block. We measured the slope efficiencies for the usable output after the isolators, neglecting Fresnel reflections and coupling losses for the diode pump. The usable average power slope efficiency of the first and second amplifier is 10% and 7% at 4 kHz repetition rate, respectively, which is similar to the decrease in efficiency as the repetition rate was reduced from 50 to 10 kHz during Q-switched operation [11]. As shown in the inset of Fig. 2, the beam quality remains near diffraction limited, corresponding to an M^2 of <1.3 similar to that measured in previous experiments [10].

It can be seen in Fig. 3 that the amplified pulses show steepening toward the leading edge at highest output powers because of the high gain in the first amplifier; however, the pulse width remains 7 ns (FWHM). The output spectrum provides no indication of strong nonlinear effects (inset of Fig. 3) although the 10 dB width of 1.8 nm

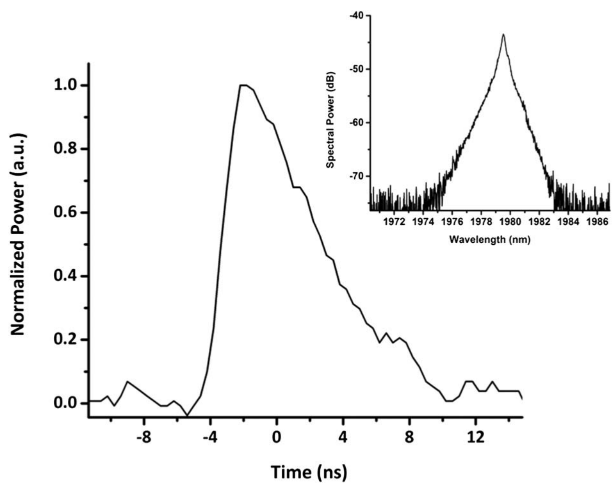

Fig. 3. Depicts the temporal shape of the output pulses at ~0.84 mJ with ~7 ns width. Inset: spectrum centered at ~1980 nm with a 10 dB width of <1.8 nm.

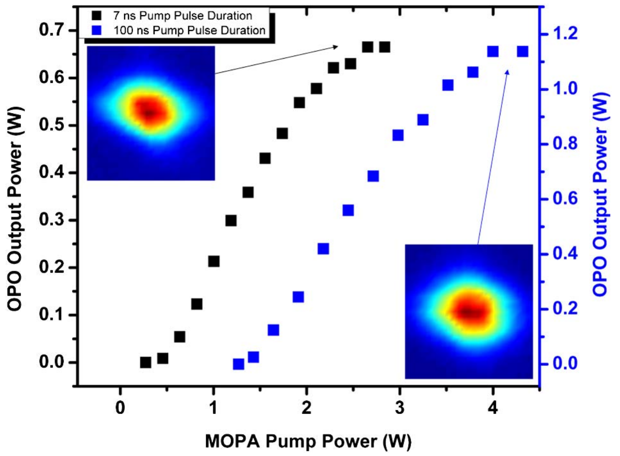

Fig. 4. DRO output for 7 and 100 ns pump pulses. The insets show the far-field beam profiles at highest powers.

is nearly twice that of the oscillator output. To pump the OPO, the output beam was demagnified to a $1/e^2$-radius of ~335 μm using a 4:1 telescope consisting of 200 and 50 mm focusing lenses. The ZGP crystal has a clear aperture of 5 mm × 4 mm and 12 mm long cut at an angle $\theta = 57.7°$ with respect to the C-axis for Type I phase matching. The OPO experiments were conducted for a doubly resonant oscillator (DRO) and a split-reflectivity DRO cavity configuration. The DRO cavity had a length of ~20 mm consisting of two flat ZnSe mirrors. The input and output coupler are coated for high transmission (HT) for the pump, with 99% and 50% reflectivity coatings for the wavelength range from 3 to 5 μm, respectively.

In two experiments the DRO was pumped with 7 and 100 ns pulses to demonstrate high mid-IR peak power and pulse energy, respectively. The results can be seen in Fig. 4. For 7 ns pump pulses, a maximum total mid-IR peak power of ~28 kW was achieved, corresponding to ~165 μJ. The maximum total mid-IR pulse energy was ~280 μJ for 100 ns pumping. The slope efficiency in the linear part of the curves reaches 38% for the short pump pulses and up to 49% for the longer pump pulses as there are more OPO cavity round trips to build up the signal and idler in the long pulse case. The OPO cavity configuration could be improved, for example by implementing a ring cavity [6] to enable >50% conversion efficiency. During OPO pumping the main limitation to the mid-IR output was parasitic lasing in the power amplifiers at about 85% of the available 2 μm pump power despite isolation and angle cleaved fiber ends. It was confirmed that the self-lasing was caused by reflection from the OPO input coupler. In this context, more advanced cavity designs mitigating this feedback such as RISTRA [13] would be beneficial for the performance of the OPO. Moreover, we estimate the presence of a significant thermal lens in the ZGP at highest pump powers using a similar method to that done by Tucker *et al.* [14]. Thus, we believe that the slight roll-off, which can be seen in the OPO output before it is limited by the self-lasing in the power amplifiers, is due to thermal lensing in the ZGP. However, the relatively low peak-intensity threshold of <5.5 MW/cm^2 provides the possibility to further scale pump energy and/or average power when increasing the spot size within the crystal. Furthermore, the output beam profiles in the far field displayed in the insets of Fig. 4 do not show any significant distortion. The combination of high energy and nearly Gaussian beam profile is well suited for materials processing experiments in the mid-IR.

The spectrum of the DRO output was analyzed using a low spectral-resolution grating-based monochromator (Oriel/Newport) demonstrating a wavelength tuning for signal and idler from 3.3 to 4.7 μm. Figure 5 shows an example of angular tuning the ZGP crystal relative to the pump's angle of incidence by about 1°. We believe that the attenuation of the idler peak at normal incidence is atmospheric absorption at ~4.2 μm due to CO_2 [15].

In order to expand the tuning range to longer idler wavelengths, we investigated a split-reflectivity DRO configuration using 7 ns pump pulses only. The cavity was again ~20 mm long and consisted of a flat input coupler that was HT for the pump and 99% reflective for 2.4–4 μm. The output coupler had the same coating but with 100 mm radius of curvature. Ideally in this configuration, the signal resonates in the cavity without significant output coupling and the corresponding, long-wave idler basically builds up in a single pass. Unfortunately, the mirrors we used had undesirably high reflectivity of >60% across the idler (>4 μm). The reflectivity of the mirrors was minimum (~25%) for a narrow wavelength window at ~4.8 μm. As such, the configuration was closest to an ideal singly resonant oscillator (SRO) at this point. The split-reflectivity DRO performance as a function of the idler wavelength is shown in Fig. 6. We observed a decreasing threshold when tuning the wavelengths of signal and idler closer to degeneracy. The slope efficiency was found to be significantly higher at an idler wavelength of ~4.85 μm. Therefore, the OPO performance at longer idler wavelengths could be improved with optimized mirrors. Another limit in this configuration is the signal fluence within the cavity, which approaches the damage threshold of ZGP reaching ~0.4 J/cm^2 at the highest output power.

In this Letter, we demonstrate a nanosecond Tm:fiber MOPA system capable of producing >100 kW of usable

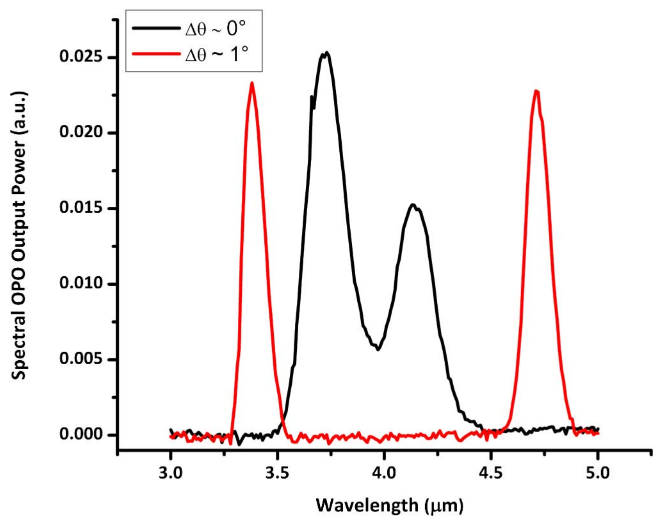

Fig. 5. Exemplarily angular tuning of the DRO output, the measurements leading to the highest output powers have been conducted at $\Delta\theta = 0°$.

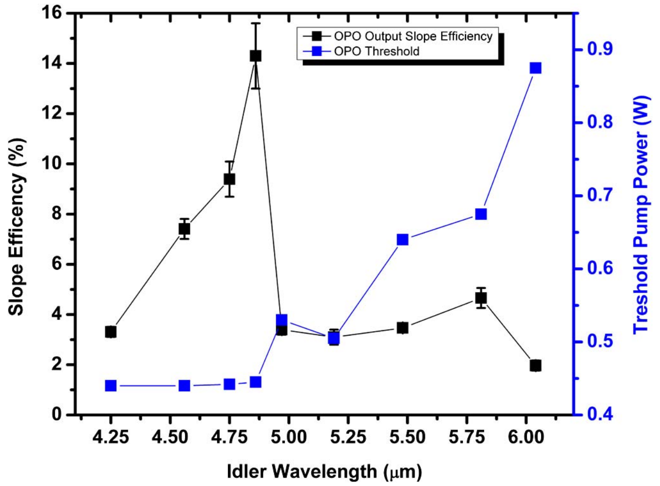

Fig. 6. Plots split-reflectivity DRO threshold and slope efficiency as a function of idler wavelength.

peak power with near diffraction-limited beam quality and polarized output. The high peak power and near ideal beam quality of the Tm:fiber MOPA system make it possible to generate a maximum mid-IR signal output at 3.7 μm with ~15 kW peak power and ~90 μJ pulse energy when pumped at 1980 nm with ~700 μJ, ~7 ns pulses. To the best of our knowledge, this is the highest reported mid-IR output peak power from a Tm:fiber laser pumped ZGP OPO and a strong improvement in terms of pulse energy as compared to the first investigations of this approach [8,9]. Significantly higher mid-IR energy is possible using Tm:PCF laser pumping based upon ultra-large mode area rod-type fibers [16,17]. However, further development is still needed to improve the efficiency, integration, and reliability of such systems. Further scaling of mid-IR output and/or higher conversion efficiency can be achieved with improved OPO cavity design.

The authors acknowledge the contribution of the ZGP crystal from BAE Systems and PCFs from NKT Photonics. This research was funded by the United State High Energy Laser Joint Technology Office (HEL JTO) through contracts FA9550-10-1-0543 and W911NF-12-1-0450, the Master International in Laser, Materials science and Interaction (MILMI) program, and the Innovative Mid-infrared high Power source for Resonant ablation of Organic based photovoltaic devices (IMPROV) grant 257894.

References

1. D. L. Snavely and J. Dubsky, J. Poly. Sci. A **34**, 2575 (1996).
2. D. N. Nikogosyan, *Nonlinear Optical Crystals: A Complete Survey* (Springer, 2005).
3. P. A. Budni, L. A. Pomeranz, M. L. Lemons, P. G. Schunemann, T. M. Pollak, and E. P. Chicklis, in *Proceedings of Advanced Solid-State Lasers* (Optical Society of America, 1998), paper FC1.
4. K. L. Vodopyanov, F. Ganikhanov, J. P. Maffetone, I. Zwieback, and W. Ruderman, Opt. Lett. **25**, 841 (2000).
5. K. Vodopyanov and P. Schunemann, Opt. Lett. **28**, 441 (2003).
6. E. Lippert, H. Fonnum, G. Arisholm, and K. Stenersen, Opt. Express **18**, 26475 (2010).
7. A. Dergachev, D. Armstrong, A. Smith, T. Drake, and M. Dubois, Opt. Express **15**, 14404 (2007).
8. D. Creeden, M. Jiang, P. A. Budni, P. A. Ketteridge, S. D. Setzler, Y. E. Young, J. C. McCarthy, P. G. Schunemann, T. M. Pollak, P. Tayebati, and E. P. Chicklis, Proc. SPIE **6952**, 69520S (2008).
9. N. Simakov, A. Davidson, A. Hemming, S. Bennetts, M. Hughes, N. Carmody, P. Davies, and J. Haub, Proc. SPIE **8237**, 82373K (2012).
10. N. Modsching, P. Kadwani, R. Sims, L. Leick, J. Broeng, L. Shah, and M. Richardson, Opt. Lett. **36**, 3873 (2011).
11. P. Kadwani, N. Modsching, R. A. Sims, L. Leick, J. Broeng, L. Shah, and M. Richardson, Opt. Lett. **37**, 1664 (2012).
12. S. D. Agger and J. H. Povlsen, Opt. Express **14**, 50 (2006).
13. A. Smith and D. Armstrong, J. Opt. Soc. Am. B **19**, 1801 (2002).
14. J. E. Tucker, C. L. Marquardt, S. R. Bowman, and B. J. Feldman, Appl. Opt. **34**, 2678 (1995).
15. J. Howard and R. Chapman, J. Opt. Soc. Am. **42**, 856 (1952).
16. C. Gaida, M. Gebhardt, P. Kadwani, L. Leick, J. Broeng, L. Shah, and M. Richardson, Opt. Lett. **38**, 691 (2013).
17. F. Stutzki, F. Jansen, C. Jaurgui, J. Limpert, and A. Tünnermann, Opt. Lett. **38**, 97 (2013).